



Perspectives on the non-invasive evaluation of femoral strength in the assessment of hip fracture risk

M. L. Bouxsein¹ · P. Zysset² · C. C. Glüer³ · M. McClung^{4,5} · E. Biver⁶ · D.D. Pierroz⁷ · S. L. Ferrari⁶ · on behalf of the IOF Working Group on Hip Bone Strength as a Therapeutic Target

Received: 23 August 2019 / Accepted: 4 October 2019 / Published online: 3 January 2020
© International Osteoporosis Foundation and National Osteoporosis Foundation 2020

Abstract

Summary We reviewed the experimental and clinical evidence that hip bone strength estimated by BMD and/or finite element analysis (FEA) reflects the actual strength of the proximal femur and is associated with hip fracture risk and its changes upon treatment.

Introduction The risk of hip fractures increases exponentially with age due to a progressive loss of bone mass, deterioration of bone structure, and increased incidence of falls. Areal bone mineral density (aBMD), measured by dual-energy X-ray absorptiometry (DXA), is the most used surrogate marker of bone strength. However, age-related declines in bone strength exceed those of aBMD, and the majority of fractures occur in those who are not identified as osteoporotic by BMD testing. With hip fracture incidence increasing worldwide, the development of accurate methods to estimate bone strength in vivo would be very useful to predict the risk of hip fracture and to monitor the effects of osteoporosis therapies.

Methods We reviewed experimental and clinical evidence regarding the association between aBMD and/or CT-finite element analysis (FEA) estimated femoral strength and hip fracture risk as well as their changes with treatment.

Results Femoral aBMD and bone strength estimates by CT-FEA explain a large proportion of femoral strength ex vivo and predict hip fracture risk in vivo. Changes in femoral aBMD are strongly associated with anti-fracture efficacy of osteoporosis treatments, though comparable data for FEA are currently not available.

Conclusions Hip aBMD and estimated femoral strength are good predictors of fracture risk and could potentially be used as surrogate endpoints for fracture in clinical trials. Further improvements of FEA may be achieved by incorporating trabecular orientations, enhanced cortical modeling, effects of aging on bone tissue ductility, and multiple sideways fall loading conditions.

Keywords Bone mineral density (BMD) · Bone strength · Finite element analysis (FEA) · Hip fracture

✉ S. L. Ferrari
serge.ferrari@unige.ch

- ¹ Center for Advanced Orthopedic Studies, Beth Israel Deaconess Medical Center, and Department of Orthopedic Surgery, Harvard Medical School, Boston, MA, USA
- ² ARTORG Center for Biomedical Engineering Research, University of Bern, Bern, Switzerland
- ³ Section of Biomedical Imaging, Department of Radiology and Neuroradiology, University Medical Center of Schleswig-Holstein, Campus Kiel, Kiel, Germany
- ⁴ Oregon Osteoporosis Center, Portland, OR, USA
- ⁵ Mary MacKillop Institute for Health Research, Australian Catholic University, Melbourne, VIC, Australia
- ⁶ Division of Bone Disease, Department of Internal Medicine Specialties, Faculty of Medicine, Geneva University Hospital, Geneva, Switzerland
- ⁷ International Osteoporosis Foundation (IOF), Nyon, Switzerland

Epidemiology of hip fractures

Globally 9 million fragility fractures were estimated to occur in the year 2000, including 1.6 million hip fractures [1]. The number of hip fractures worldwide is estimated to increase 3 to 4-fold by 2050 [2, 3]. Those who suffer a hip fracture exhibit marked reductions in mobility, independence, quality of life, and survival. Moreover, hip fractures represent the highest burden of osteoporosis on health care systems and costs [4]. The life-time risk of a hip fracture at the age of 50 years is in the order of 3 to 23% in men and women, with wide variations worldwide [5–8]. Following a hip fracture, the risk of suffering another hip fracture is increased 2-fold in women and 3-fold in men [9], with rates up to 5% within 1 year and 10% within 10 years, whereas the rates of another peripheral fragility fracture are approximately 7% at 1 year and up to

28% at 10 years [10, 11]. Yet, secondary fracture prevention after a hip fracture is prescribed in only 10 to 40% of these patients [12, 13]. In this context, the development and the implementation of coordinated-based systems for secondary fracture prevention, as for example Fracture Liaison Services (FLS) and Capture the Fracture® from the International Osteoporosis Foundation (IOF), is beneficial to ensure appropriate care of fracture patients [14–16].

This exponential increase in hip fracture risk with aging is the result of a progressive loss of bone mass and structural and material deterioration of trabecular and cortical bone combined with other non-skeletal disorders leading to more frequent falls. Areal bone mineral density (aBMD) as measured by dual-energy X-ray absorptiometry (DXA) is the most commonly used surrogate of bone strength, and low aBMD is strongly associated with increased fracture risk in untreated patients [17]. However age-related changes in bone microstructure, including trabecular thinning and loss of connectivity, and specifically regarding the hip, asymmetrical cortical thinning [18] and increased cortical porosity [19], lead to a greater loss of estimated bone strength than aBMD [20].

The relationship between changes in aBMD and fracture risk reduction during osteoporosis therapies has, through evidence from individual studies [21] as well as the meta-analysis from the FNIH Bone Quality Study, indicated that improvements in hip aBMD with treatment are strongly associated with reductions in fracture risk, particularly for hip fractures [22, 23]. Therefore, the development of accurate methods to estimate bone strength in vivo could improve our ability to predict hip fracture risk and monitor the effects of interventions designed to reduce fractures.

Here, we review the experimental and clinical evidence that hip bone strength estimated by BMD and/or finite element analysis (FEA) reflects the actual strength of the proximal femur and is associated with hip fracture risk and its changes upon treatment.

Associations between experimentally measured femoral strength and areal BMD or FEA-estimated strength

There is extensive evidence from human cadaveric studies that hip aBMD and FEA estimates of femoral strength correlate strongly with ex vivo strength of the proximal femur in both stance and fall configurations. The stance configuration corresponds to the single-leg stance phase of walking, whereas the fall configuration mimics a sideway fall with impact to the greater trochanter.

In stance configuration, femoral strength ranges from 2 to 16 kN and is consistently lower in women than in men [24, 25]. In the stance loading configuration, most fractures are of cervical type (Table 1). In comparison, femoral strength in the

fall configuration is approximately half of that in the stance configuration, ranging from 1 to 10 kN (Table 1). Further, femoral strength is sensitive to the loading rate and loading direction, increasing by 18% when the loading rate increases from 120 to 6000 mm/min and decreasing by approximately 25% when increasing the angle in the transverse plane from 0 to 30° [37]. In the fall loading configuration, fractures are more balanced between cervical and trochanteric types, thus corresponding better to the clinical observations. Interestingly, a larger proportion of intertrochanteric fractures occur with lower hip strength [39, 51]. The strength of femurs from old donors (mean age of 74 ± 7 years) is approximately 50% lower than those from young donors (mean age 32 ± 13) [36]. Assuming perfect symmetry between left and right femora, the precision error of the femoral strength testing in the fall configuration is approximately 15% [52]. Since real hip fractures do not occur at constant displacement or load rates as applied in standard testing machines, recent studies have used a drop tower to produce more realistic hip fractures ex vivo [47, 49]. Unfortunately, these tests seem to be less reproducible, as small differences in the loading protocol lead to large differences in the outcome variables [47].

Surrogates of hip strength: densitometric and structural variables

Multiple surrogates of in vitro bone strength have been explored over the past decades, starting with bone mineral content (BMC), aBMD, or volumetric (v) BMD obtained by DXA and quantitative computed tomography (QCT), respectively. Geometrical variables such as the cross-sectional area (CSA) or neck length have also been examined, as has DXA-based hip structure analyses (HSA) [26].

In the stance configuration, various DXA-aBMD measures from the proximal femur are strongly associated with femoral strength ($R^2 = 0.51$ to 0.66 , Tables 2 and 3). A few studies report that the prediction of femoral strength can be improved by combining aBMD with femoral geometry assessed by hip structural analysis (HSA) (R^2 increases from 0.63 to 0.79) [26] and with incorporation of tissue level material properties assessed by microindentation (R^2 increases from 0.57 to 0.78) [57]. CT-based integral vBMD is also strongly associated with femoral strength ($R^2 = 0.55$ to 0.64). The multiplicative combination of integral vBMD with CSA increases the correlation from $R^2 = 0.61$ to 0.82 [59]. The association between BMC and femoral strength is more variable, with R^2 between 0.45 and 0.79.

In the fall configuration, DXA-aBMD is more strongly associated with femoral strength than in the stance configuration, with R^2 values ranging from 0.61 to 0.94 (Tables 2 and 3). This is also the case in a direct comparison of fall vs stance loading within the same donors (using contralateral femurs), where DXA-aBMD delivers

Table 1 Ex vivo hip strength: stance and sideways fall configurations

Sample size and sex distribution	Age	Rate [mm/min]	Config [°]	Strength [kN]	Loc [% cervical fracture]	Reference
11F* + 11M	34–90	5	sta 0	2–13.5	95	Beck et al., 1990 [26]
22	–	13	sta 24	4.94–16.15	–	Smith et al., 1992 [27]
24F*	84 ± 10	60	sta 0	2.25 ± 0.88	–	Lochmüller et al., 1998 [24]
34M*	81 ± 9	60	sta 0	3.79 ± 1.06	–	Lochmüller et al., 1998 [24]
23F + 28M	21–93	13	sta 25	9.55 ± 3.20	87	Cody et al., 1999 [28]
10F + 8M	52–92	30	sta 20	3.2–15.0	100	Keyak et al., 2001 [29, 30]
7F + 13M	48–92	10	sta 12	5.3–14.5	100	Kukla et al., 2002 [31]
6F + 5M	30–90	0.5	sta 20	5.45 ± 1.02	100	Bessho et al., 2007 [32]
1F + 11M	51–83	120	sta 8	6.32–16.04	100	Cristofolini et al., 2007 [33]
24F + 16M	47–100	13	sta 25	8.87 ± 3.32	–	Duchemin et al., 2008 [34]
19F + 17M	46–96	5	sta 20	8.71 ± 2.93	78	Dall'Ara et al., 2013 [35]
4F + 6M	74 ± 7	6000	fa 80, 15	4.13 ± 1.62	56	Courtney et al., 1994 [36]
4F + 6M	74 ± 7	120	fa 80, 15	3.50 ± 1.38	–	Courtney et al., 1994 [36]
10F	32 ± 13	6000	fa 80, 15	7.87 ± 1.50	67	Courtney et al., 1994 [36]
11	Elderly	6000	fa 80, 0	4.05 ± 0.90	–	Pinilla et al., 1996 [37]
11	Elderly	6000	fa 80, 15	3.82 ± 0.91	–	Pinilla et al., 1996 [37]
11	Elderly	6000	fa 80, 30	3.06 ± 0.89	–	Pinilla et al., 1996 [37]
28F + 36M	69 ± 15	840	fa 80, 15	3.98 ± 1.6	41	Cheng et al., 1997 [38]
10F + 8M	52–92	30	fa 60, 20	2.31 ± 1.27	37	Keyak et al., 2001 [29, 30]
77F* + 63M	80.5	396	fa 80, 15	2.62–4.57	63	Pulkkinen et al., 2006 [39]
17F + 10M	73 ± 13	6000	fa 80, 15	4.34 ± 1.91	23	Manske et al., 2009 [40]
6F + 6M	72–93	6000	fa 80, 15	4.03 ± 0.37	50	de Bakker et al., 2009 [41]
48F + 25M	55–98	6000	fa 80, 15	3.57 ± 1.82	–	Roberts et al., 2010 [42]
13F + 5M	51–93	6000	fa 80, 15	1.41–6.18	44	Dragomir-Daescu et al., 2011 [43]
41F* + 20M	55–100	396	fa 80, 15	3.53 ± 1.07	–	Koivumäki et al., 2012 [44]
19F + 17M	46–96	5	fa 60, 0	3.12 ± 1.14	78	Dall'Ara et al., 2013 [35]
15F + 5M	77 ± 13	120	fa 80, 15	~ 1.3–4.4	–	Nishiyama et al., 2013 [45]
37F + 28M	67 ± 14	120	fa 80, 15	3.15 ± 1.15	25	Gebauer et al., 2014 [46]
15F + 2M	77 ± 11	Free fall	fa 80, 15	1.41–3.72	–	Gilchrist et al., 2014 [47]
8F + 3M	59–84	930–2970	fa 80, 15	3.18 ± 1.46	27	Zani et al., 2015 [48]
10F + 4M	72–95	Free fall	fa 80, 15	3.36 ± 1.25	–	Varga et al., 2016 [49]
24F + 16M	82 ± 12	13	fa 80, 15	2.48 ± 1.21	–	Pottecher et al., 2016 [50]
50F + 26M	74 ± 9	6000	fa 80, 15	3.58 ± 1.48	24	Johannesdottir et al., 2017 [25]
128F + 69M	69 ± 14	300	fa 80, 15	~ 0.8–10	46	Dragomir-Daescu et al., 2018 [51]
		6000	fa 80, 30			
		42,000	fa 70, 15			
			fa 70, 30			

Config, stance (sta) or fall (fa) with angle of applied force with respect to the femoral shaft in the neck-shaft plane; *Loc*, the fraction of cervical versus trochanteric fractures

*Bones were fixed

$R^2 = 0.66$ for stance and $R^2 = 0.80$ for the fall loading configuration [35]. In an initial study, CT-based vBMD was strongly correlated with femoral strength ($R^2 = 0.87$) [58], but notably this strong association could be reproduced in later studies or by the combination of vBMD and CSA [59].

Overall, DXA-based hip aBMD ex vivo is a good predictor of femoral strength in stance and to an even higher

extent in the sideways fall configurations [39]. However, the predictive equations depend significantly on sex and age, leading to a global correlation coefficient of $R^2 = 0.78$ in the fall configuration [51]. There is no added value in using CT-based variables and the inclusion of geometrical variables improves the predictions rather moderately.

Table 2 Prediction of ex vivo hip strength in the stance and fall configurations: densitometric variables alone (no FEA data available)

Sample size and sex distribution	Age	Loading configuration	Variables	R ²	Reference
54F + 7M	67–80	Stance	FN BMC	0.79	Dalen et al., 1976 [53]
9F + 9M	32–83	Stance	vBMD	0.66	Leichter et al., 1982 [54]
4F + 4M	62–92	Stance	HU	0.64	Esses et al., 1989 [55]
11F + 11M	34–90	Stance	FN aBMD	0.63	Beck et al., 1990 [26]
11F + 11M	34–90	Stance	FN aBMD + HSA	0.79	Beck et al., 1990 [26]
22	–	Stance	vBMD	0.55	Smith et al., 1992 [27]
24F + 34M	57–100	Stance	FN BMC	0.45	Lochmüller et al., 1998 [24]
7F + 13M	48–92	Stance	tot hip aBMD	0.62	Kukla et al., 2002 [31]
7F + 13M	48–92	Stance	troch aBMD	0.66	Kukla et al., 2002 [31]
7F + 13M	48–92	Stance	FN aBMD	0.51	Kukla et al., 2002 [31]
14F + 17M	29–91	Stance	FN aBMD	0.55	Link et al., 2003 [56]
28F	57–97	Stance	aBMD	0.57	Abraham et al., 2015 [57]
28F	57–97	Stance	aBMD + μ ind	0.78	Abraham et al., 2015 [57]
5F + 7M	53–81	Sideway fall	vBMD	0.87	Lotz and Hayes, 1990 [58]
4F + 6M	73.8 ± 7.1	Sideway fall	FN aBMD	0.72	Courtney et al., 1994 [36]
4F + 6M	73.8 ± 7.1	Sideway fall	CSA	0.77	Courtney et al., 1994 [36]
33	Elderly	Sideway fall	tot hip aBMD	0.69	Pinilla et al., 1996 [37]
28F + 36M	69 ± 15	Sideway fall	troch aBMD	0.88	Cheng et al., 1997 [38]
28F + 36M	69 ± 15	Sideway fall	troch CoA	0.83	Cheng et al., 1997 [38]
17F + 10M	73 ± 13	Sideway fall	FN aBMD	0.64	Manske et al., 2009 [40]
17F + 10M	73 ± 13	Sideway fall	FN CoA	0.69	Manske et al., 2009 [40]
48F + 25M	74 ± 9	Sideway fall	FN aBMD	0.70	Roberts et al., 2010 [42]
37F + 28M	67 ± 14	Sideway fall	troch aBMD	0.54	Gebauer et al., 2014 [46]
37F + 28M	67 ± 14	Sideway fall	tot hip vBMD	0.30	Gebauer et al., 2014 [46]
15F + 2M	77 ± 11	Sideway fall	tot hip aBMD	0.39	Gilchrist et al., 2014 [47]
19F + 1M	77 ± 10	Sideway fall	tot hip aBMD	0.94	Gilchrist et al., 2014 [47]

BMD, bone mineral density; BMC, bone mineral content; HAS, hip structure analysis; HU, Hounsfield units; FN, femoral neck; troch, trochanter; v, volumetric; a, areal; μ ind, microindentation; CSA, cross-sectional area; CoA, cortical area by CT; tot, total

Surrogates of hip strength: finite element analysis

In contrast to densitometric variables, finite element analysis (FEA) integrates the bone geometry, and heterogeneous distribution of bone density, using first equilibrium principles to directly compute mechanical variables such as stiffness, ultimate load, and energy to failure for a given load configuration [70]. Such computations may be done on a simplified 2D projection by using DXA images (DXA-FEA) [71, 72] or on a full 3D geometry by using either QCT data (CT-FEA) [28, 59, 73] or 2D-3D reconstructions from DXA images [74, 75]. In the common approaches, the geometry of the femur is divided into finite elements that form a mesh. The material properties of the bone tissue are determined by using the vBMD in the neighborhood of each element and validated using in vitro tests to achieve a reasonable correspondence between experimental and computational strength. Precision of stiffness using linear CT-FEA of the hip in stance is reported to be by 1.85% [76], which is about twice the typical precision of 1% reported for densitometric variables such as vBMD. For DXA-FEA, the precision is in the range of 5–7% for several fracture risk indices [71].

The strength of the association between ex vivo femoral strength and CT-based FEA ($R^2 = 0.75$ – 0.96) is consistently

higher than that obtained by densitometric variables (Table 3), and appears to improve with the resolution of the underlying QCT image [68]. The application of the FE approach on 2D DXA images provided coefficients of determination higher than those of aBMD for stance configuration ($R^2 = 0.74$ versus $R^2 = 0.66$), but similar to those of aBMD for the fall configuration ($R^2 = 0.77$ versus $R^2 = 0.80$). The predictions of hip strength achieved with 2D DXA-based FEA remain inferior to the ones of 3D CT-based FEA [77]. In a precision study, it was shown that 2D FE methods based on DXA suffer from a significant variability due to positioning of the patient during the examination [71]. A recent development attempts to build 3D FE models from standard radiographs [66]. Although the strategy appears attractive, the first results were not fully convincing with a coefficient of determination of $R^2 = 0.64$, but much better than those of aBMD ($R^2 = 0.24$), which may indicate inconsistencies in the experimental boundary conditions. The ongoing research on 2D-3D reconstruction of the proximal femur from DXA images may open new perspectives in this field [75, 78].

Overall, the prediction error for hip strength by FEA evaluated ex vivo remains between 10 and 20% [79], similar to the one for aBMD [80]. Unlike aBMD, FEA can predict ex vivo hip strength in stance and fall similarly [67]. It remains unclear whether accounting for tissue age in FE modeling could

Table 3 Prediction of hip strength ex vivo: densitometry and FEA

Sample size and sex distribution	Age	Loading configuration	Variables	R ²	Reference
10F + 8M	52–92	Stance	neck vBMD	0.61	Keyak et al., 1998 [59]
10F + 8M	52–92	Stance	lin FE	0.75	Keyak et al., 1998 [59]
10F + 8M	52–92	Fall	vBMD × CSA	0.82	Keyak et al., 1998 [59]
10F + 8M	52–92	Fall	lin FE	0.90	Keyak et al., 1998 [59]
10F + 8M	52–92	Stance	nonlin FE	0.93	Keyak et al., 2001 [29, 30]
23F + 28M	21–93	Stance	aBMD	0.57	Cody et al., 1999 [28]
23F + 28M	21–93	Stance	lin FE	0.84	Cody et al., 1999 [28]
6F + 5M	30–90	Stance	nonlin FE	0.96	Bessho et al., 2007 [32]
24F + 16M	47–100	Stance	lin FE	0.87	Duchemin et al., 2008 [34]
9	74–91	Stance	lin FE	0.94	Pithioux et al., 2011 [60]
13F + 5M	51–93	Fall	aBMD	0.78	Dragomir-Daescu et al., 2011 [43]
13F + 5M	51–93	Fall	nonlin FE	0.85	Dragomir-Daescu et al., 2011 [43]
41F + 20M	55–100	Fall	nonlin FE	0.87	Koivumäki et al., 2012 [44]
19F + 17M	46–96	Stance	aBMD	0.66	Dall'Ara et al., 2013 [35]
19F + 17M	46–96	Stance	nonlin FE	0.80	Dall'Ara et al., 2013 [35]
19F + 17M	46–96	Stance	nonlin FE	0.87	Luisier et al., 2014 [62]
19F + 17M	46–96	Fall	aBMD	0.80	Dall'Ara et al., 2013 [61]
19F + 17M	46–96	Fall	nonlin FE	0.85	Dall'Ara et al., 2013 [61]
19F + 17M	46–96	Fall	nonlin FE	0.86	Luisier et al., 2014 [62]
15F + 5M	77 ± 13	Fall	lin FE	0.81	Nishiyama et al., 2013 [45]
7F + 3M	32–100	Stance	nonlin FE	0.94	Hambli and Allaoui, 2013 [63]
10F + 8M	52–92	Stance	2D FE	0.80	Langton et al., 2009 [64]
7	55–95	Fall	lin FE	0.35	Enns-Bray et al., 2014 [65]
28	–	Stance	aBMD	0.24	Thevenot et al., 2014 [66]
28	–	Stance	2D-3D FE	0.64	Thevenot et al., 2014 [66]
1F + 6M	71–83	Stance	lin FE	0.54	Schileo et al., 2014 [67]
6F + 1M	62–84	Fall	lin FE	0.77	Schileo et al., 2014 [67]
7F + 7M	62–84	Both	lin FE	0.89	Schileo et al., 2014 [67]
8F + 4M	62–93	Fall	aBMD	0.61	Nawathe et al., 2014 [68]
8F + 4M	62–93	Fall	nonlin μ FE	0.94	Nawathe et al., 2014 [68]
14F + 1M	50–96	Fall	explicit FE	ns	Ariza et al., 2015 [69]
10F + 4M	72–95	Fall	nonlin FE	0.84	Varga et al., 2016 [49]
24F + 16M	82 ± 12	Fall	troch aBMD	0.80	Pottecher et al., 2016 [50]
24F + 16M	82 ± 12	Fall	troch BMC	0.79	Pottecher et al., 2016 [50]
24F + 16M	82 ± 12	Fall	lin FE	0.83	Pottecher et al., 2016 [50]
50F + 26M	74 ± 9	Fall	tot aBMD	0.74	Johannesdottir et al., 2017 [25]
50F + 26M	74 ± 9	Fall	tot CoV	0.74	Johannesdottir et al., 2017 [25]
50F + 26M	74 ± 9	Fall	nonlin FE	0.79	Johannesdottir et al., 2017 [25]

BMD, bone mineral density; *BMC*, bone mineral content; *v*, volumetric; *a*, areal; *lin*, linear; *nonlin*, nonlinear; *FE*, finite element; *CSA*, cross-sectional area; *CoV*, cortical volume; *troch*, trochanter; *tot*, total

improve these predictions. Of interest, FEA is also able to predict fracture location (e.g., cervical versus trochanteric) with reasonable to excellent accuracy (61 to 100%) [79].

In summary, ex vivo biomechanical tests provide robust measures of femoral strength in clinically relevant loading conditions. Validation of surrogate measures of femoral strength derived from non-invasive imaging strength shows that whereas DXA-based aBMD is strongly associated with femoral strength, 3D QCT-based FEA consistently provides slightly better predictions of ex vivo femoral strength than densitometric or other structural variables. DXA-based 2D-FEA estimates of bone strength provide similar associations with femoral strength as aBMD, but suffer somewhat from higher precision errors. Though still being developed, 2D-3D densitometric reconstruction of the proximal femur from DXA images followed

by FEA should be investigated further to determine whether it can overcome the current limitations of aBMD.

Clinical studies: prediction of hip fracture by FEA

CT- and DXA-based FEA of the proximal femur have been evaluated in a number of prospective studies, demonstrating significant associations with hip fracture risk, sometimes independently of aBMD (Table 4). Generally the associations between femoral strength and hip fracture are as strong if not stronger than those reported for aBMD, though only one study was able to demonstrate statistically significantly stronger predictive power for hip fractures by CT-FEA compared to aBMD in women [84].

Table 4 Summary of selected studies using aBMD or QCT-based FE for the prediction of hip fracture in humans

Study name	Study population	Number of incident hip fractures	Techniques	HR or odds ratio for incident hip fracture (and 95% confidence intervals)	Reference
Nested case-control study design	728 women ≥ 75 years of age 4 years of follow-up	182	DXA-based FE	TH aBMD: 1.8 (1.5–2.1) FN aBMD: 2.1 (1.7–2.6) Strength: 2.2 (1.8–2.8) Strength***: 1.7 (1.2–2.4) Load-to-strength ratio: 1.8 (1.5–2.1) Load-to-strength ratio***: 1.4 (1.1–1.7)	Naylor et al., 2013 [81]
SOF	2609 women ≥ 67 years of age 12.8 years follow-up	668	DXA-based FE	TH aBMD: 1.9 (1.7–2.1) [⊕] FN aBMD: 2.0 (1.8–2.3) [⊕] Strength: 2.2 (2.0–2.5) [⊕]	Yang et al., 2014 [72]
MrOs	250 men ≥ 65 years of age 5.6 years follow-up	40	QCT-based FE	TH aBMD: 4.4 (2.1–9.1)* Strength: 6.5 (2.3–18.3)* Load-to-strength ratio: 4.3 (2.5–7.4)*	Orwoll et al., 2009 [82]
AGES Reykjavik	608 women and 440 men ≥ 65 years of age 5 years follow-up	171	QCT-based FE	<i>Women</i> [⊕] TH aBMD: 2.6 (1.8–3.8) FN aBMD: 2.7 (1.8–4.0) Strength: 4.3 (2.6–7.4) Load-to-strength ratio: 2.3 (1.8–3.0) <i>Men</i> [⊕] TH aBMD: 2.8 (1.9–4.1) FN aBMD: 4.0 (2.6–6.1) Strength: 3.7 (2.4–5.7) Load-to-strength ratio: 2.6 (1.9–3.5)	Kopperdahl et al., 2014 [83]
FOCUS	2690 women and 1248 men ≥ 65 years of age	1959	QCT-based FE	<i>Women</i> [°] DXA-based hip aBMD: 2.1 (1.7–2.5) CT-derived hip aBMD: 2.1 (1.8–2.5) Strength: 2.8 (2.2–3.5) <i>Men</i> [°] DXA-based hip aBMD: 2.5 (2.0–3.2) CT-derived hip aBMD: 2.8 (2.1–3.8) Strength: 2.8 (2.1–3.7)	Adams et al., 2018 [84]
Manitoba BMD Registry	13,978 women and men ≥ 50 years of age	268	DXA-based FE to calculate site-specific FRI	FRI femoral neck***: 1.9 (1.7–2.2)	Leslie et al., 2019 [85]

TH, total hip; FN, femoral neck; BMI, body mass index; HR, hazard ratio; DXA, dual X-ray absorptiometry; FE, finite element; QCT, quantitative computed tomography; FRI, fracture risk indices

*Adjusted for age, BMI, and left

**Adjusted for FN aBMD

***Adjusted for age and sex

[⊕] Adjusted for age and BMI

[°] Adjusted for age, race/ethnicity, and BMI

Predictive power for hip fracture of CT-based FE approaches

The ability of CT-FEA femoral strength to predict hip fracture was first reported in the MrOs Study, a population-based cohort study of osteoporosis in men. In 2009, Orwoll et al. [82] used a

case-cohort design in 250 men, 40 of whom had suffered an incident hip fracture during a follow-up time of 5.6 years. In this study, bone strength (defined as ultimate failure load) was selected as the primary predictor variable but other FE-based measures were also tested, specifically the load-to-strength ratio. This ratio considers the notion that impacting loads during a

fall are related to height and weight, as well as the energy-attenuation by trochanteric soft tissues [86]. Theoretically, a load-to-strength ratio of greater than one would indicate a high risk of fracture. In the MrOs analysis, all standardized hazard ratios (sHR) were adjusted for age, BMI, and clinic center. aBMD was associated with hip fracture, with a standardized hazard ratio (sHR) of 4.4 (95% CI 2.1–9.1). Notably, FEA-based femoral strength showed a numerically higher sHR of 6.5 (95% CI 2.3–18.3). However, the difference compared to aBMD did not achieve statistical significance, potentially due to limited statistical power. The load-to-strength ratio showed a sHR = 4.3 (2.5–7.4), i.e., not better than aBMD, but was limited by use of a uniform soft tissue thickness value for all subjects.

The second prospective study investigating ability of CT-FEA to predict hip fracture was conducted in the AGES Reykjavik cohort. Fifty-one men and 77 women suffered hip fractures during a follow-up period of 4–7 years and 97 men and 152 women were selected as controls. Four loading conditions were studied: single-limb stance, stimulating loading from falls onto the posterolateral, posterior, and lateral aspects of the greater trochanter. Analyzing FE-based bone strength under different loading conditions, Keyak et al. reported age-related declines in femoral strength, along with lower bone strength in subjects with fractures [87]. Unfortunately, this study did not report hazard ratios.

Kopperdahl et al. reported strong associations between femoral strength from CT-FEA and hip fracture risk prediction in the AGES cohort, both for men and women [83]. The rationale for gender-specific analyses relates to differences in body size and BMD reference data which may lead to different threshold considered for male and female patients at high risk of fracture. Following a case-control study design, they analyzed 1110 women and men over age 65 years followed for 5 years with 171 incident hip fractures. The risk ratios for men were similar to those reported from the MrOs study: the age- and BMI-adjusted sRR for CT-FEA-based femoral strength was 3.7 (95% CI 2.4–5.7), numerically in between sRRs for aBMD of the femoral neck and the total hip (Table 4) with no statistically significant differences. Of note, aBMD was not measured by DXA but calculated from QCT data [88]. Again, the load-to-strength ratio did not perform as well as failure load, though use of a constant soft tissue thickness may have obscured important subject-specific differences in the fall loading estimates. The association between CT-FEA femoral strength and hip fracture was slightly stronger in women than men, with sRR = 4.3 (95% CI 2.6–7.4). The associations were numerically higher than those observed for DXA-aBMD of the femoral neck [sRR = 2.7 (95% CI 1.8–4.0)] and the total hip [sRR = 2.6 (95% CI 1.8–3.8)] but did not reach statistical significance. However, in a reclassification analysis for women, the combination of FEA-based strength and aBMD results showed better fracture prediction compared to aBMD alone.

The most recent and largest study investigating FEA prediction of hip fracture to date is the Fracture, Osteoporosis, and CT

Utilization Study (FOCUS) published by Adams et al. in 2018 [84]. In this retrospective case-cohort study preexisting, anonymized clinical data from electronic health records were analyzed to predict incident hip fracture. The study included men and women 65 or older who had a prior abdomen or pelvis CT scan, a DXA within 3 years of the CT, and no prior hip fracture. CT scans of the abdomen or pelvis had been acquired on 80 different CT scanners, for various reasons unrelated to the assessment of osteoporosis. Since a calibration phantom had not been scanned along with the patient, an internal calibration procedure based on contrast between air and hip fat was performed to transform CT numbers into bone density results [89]. FEA was performed following the same approach used in the MrOs study [82], and in the analysis of the AGES Reykjavik study published by Kopperdahl et al. [83]. Comparing the 1959 cases with an incident hip fracture to their non-fractured controls ($n = 1979$), FEA-based bone strength showed the strongest association with hip fracture, with an sRR = 2.8 (95% CI 2.2–3.5) for women and, almost identical, sRR = 2.8 (95% CI 2.1–3.7) for men. Interestingly, as in the AGES study data reported previously by Kopperdahl et al., the associations of DXA-based aBMD data of the proximal femur (lowest T-score of the femoral neck and the total hip) and hip fracture were stronger for men at sRR = 2.5 (95% CI 2.0–3.2) than for women at sRR = 2.1 (95% CI 1.7–2.5), and thus the difference in performance between FE-based bone strength and DXA-based aBMD was statistically significant for women but not for men. This study is important for several reasons. First of all, for the first time, a statistically significant advantage of CT-based FE analysis of bone strength compared to the current clinical standard method of DXA of the proximal femur was demonstrated, even if only for women at this stage. This complements earlier study results by Wang et al. [90] reported from the MrOS study for CT-FEA assessment of vertebral strength which reported superior performance in the prediction of incident vertebral fractures for FE-based bone strength compared to DXA-based aBMD of the spine. Second, from a practical point of view, superior fracture prediction by CT was achieved without simultaneous CT calibration for bone densitometry. This permits retrospective or concomitant analysis of CT scans covering the proximal femur ordered for reasons other than osteoporosis. Thus, information on osteoporotic fracture risk and identification of patients at high risk of fracture is feasible without additional radiation exposure. Some aspects need to be considered though. Most importantly, the use of contrast agents not only leads to bias in the measured data (that perhaps can in part be adjusted for) but this bias also reduced the predictive power to a small extent. Still, contrast enhanced CT examinations were shown to be predictive of hip fracture but, from the data presented by Adams et al, it appears that such CT examinations may not show an advantage over DXA with regard to risk prediction. Other issues remain to be investigated, including the choice of the CT scanning protocol with regard to slice

thickness (slice thickness above 3 mm may be disadvantageous) and X-ray energy and choice of reconstruction kernel (Adams et al.'s data limited to 120 kVp and standard reconstruction kernels). Also, the impacts of the type of calibration (internal as in the study by Adams et al. or asynchronous or simultaneous) remain to be investigated. Nevertheless, this groundbreaking study provided strong evidence in support of the use of clinical CT scans for skeletal health assessments.

FEA provides other advantages beyond improved fracture prediction. In the context of fracture risk assessment, the interpretation of strength is more intuitive and clinically relevant than areal density or T-scores. Failure load levels of the femur can be calculated for specific loading configurations and be compared with estimated forces for likely fall settings. It has been proposed that femoral strength values of 3000 N and 3500 N might reflect a critical level of “fragile bone strength” for women and men, respectively [83]. Patients for whom FEA indicates failure loads below this level might be the ones with high risk for fracture. Indeed, data calculated from the MrOs study [82] demonstrate that only few patients with failure loads below 3500 N did not experience a hip fracture. Such a threshold might be the FEA equivalent of the DXA-aBMD T-score level of -2.5 used for definition of osteoporosis and could be used to initiate treatment. Whether a combination of both criteria (i.e., aBMD and FEA strength) would further improve the sensitivity and specificity for identification of those at highest risk for fracture remains to be investigated, with some results already provided in the study of Adams et al. [84].

The ability to calculate femoral strength for different fall scenarios represents an advantage of FEA but also complicates the application. Keyak et al. calculated strength levels for three different fall configurations [87]. As can be seen in Fig. 1, strength levels are higher in men compared to women, and higher in

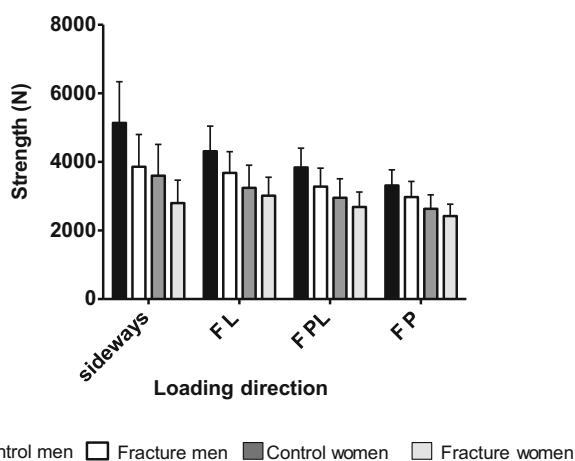


Fig. 1 Quantitative computer tomography (QCT) and finite element (FE)-based hip fracture risk prediction, adapted from Keyak et al. [87] for falls on the lateral (FL), posterolateral (FPL), and postero (FP) loading direction and Kopperdahl et al. [83] for sideways falls (using an FE method that differed from that used by Keyak et al. which makes it difficult to compare the data of the two studies)

controls compared to those with hip fracture. Femoral strength was highest for falls in a lateral direction, followed by falls in a posterolateral loading, and lowest (i.e., weakest, highest risk) for posterior loading. For comparison, the loading scenario of a sideways fall calculated by Kopperdahl [83] is also shown. The ranking within each group is the same, but there is substantial overlap between the loading scenarios. In practice, one does not know in which direction the patient is likely to fall, although some age-related patterns of typical falls have been reported. Elderly subjects tend to fall backwards, leading to posterior loading, whereas younger subjects move faster and thus experience falls more directed towards a forward direction. One interesting concept has been proposed by Bessho et al. [32]. These authors suggested to calculate strength for a variety of loading conditions to identify the patient-specific weakest scenario, i.e., the loading directions under which the proximal femur is most vulnerable to fracture. Indeed, a small case-control study (22 postmenopausal women with recent hip fracture compared to 33 non-fracture controls) used CT-FEA to compute femoral strength for a variety of sideways fall loading conditions and found that the “weakest” femoral strength tended to discriminate hip fracture cases from controls than femoral strength from the standard sideways fall configuration [91]. Potentially, application of this approach might lead to improved predictive power, a hypothesis to be tested in prospective studies.

Predictive power for hip fracture of DXA-based FE approaches

Several DXA-based structural engineering models of the proximal femur have been developed to assess bone strength and their association with hip fracture risk, though few have been tested in prospective studies.

The ability of 2D FE models generated from the segmented BMD map extracted from DXA scans to predict hip fracture was reported in two prospective studies. The first one was a nested case-control study of 728 elderly community-dwelling women (mean age 82 years), including 182 with subsequent hip fracture, selected from a large, single-center study investigating the effect of clodronate on fracture risk. Baseline DXA scans of the hip were used to determine femoral bone strength and load-to-strength ratio, which both predicted hip fracture independently of femoral neck (FN) aBMD (adjusted OR 1.7, 95% CI 1.2–2.4 and 1.4, 95% CI 1.1–1.7, respectively). However, the magnitude of the improvement of fracture discrimination was marginal compared to FN aBMD (area under the curve FN aBMD alone 0.66, FN aBMD + femoral bone strength 0.67, FN aBMD + load-to-strength ratio 0.68). DXA-based FE femoral strength was also able to discriminate incident hip fracture cases from controls independently of prior fractures including morphometric fractures, and of FRAX score (without BMD) [81]. A larger prospective case-cohort from the

Study of Osteoporotic Fractures study included 2314 women including 668 with incident hip fracture which occurred during a mean follow-up of 12.8 ± 5.7 years. In analyses adjusted for age and BMI, estimated femoral strength from 2D FE analysis of DXA scans was a strong predictor of hip fracture (HR 2.21, 95% CI 1.95–2.50). Its ability to discriminate women with and without fracture were significantly better than those of total hip aBMD and FRAX, but as in the previous study not better than FN aBMD [72]. It should be noted that strong correlations were observed between FE-estimated femoral strength and aBMD (0.81 and 0.83 for total hip and FN aBMD, respectively), which may explain the lack of improvement of fracture discrimination compared to aBMD. Another software tool that automatically performs FEA on DXA hip scans to generate site-specific (femoral neck, intertrochanteric, and subtrochanteric) fracture risk indices (FRIs) that reflect the likelihood of hip fracture from a sideways fall was tested in the Manitoba BMD Registry. Cross-sectional data showed that FRIs were able to stratify prior hip fracture risk independent of aBMD and FRAX score [92]. However, a longitudinal analysis of incident fracture discrimination determined by c-statistics in this registry showed that FRI tended to be slightly lower than femoral neck aBMD T-score and FRAX score [85].

Since these two-dimensional approaches ignore variations of geometry, bone density, and impact force in the anterior-posterior direction, DXA-based 3D modeling of the proximal femur, generated from the two-dimensional DXA scans, has been developed to generate three-dimensional FE models [64, 75, 93]. A cross-sectional case-control study of 62 hip fracture cases and 49 non-fracture controls showed that DXA-based 3D FE models of proximal femur was able to discriminate hip fracture cases versus controls, to a higher extent than aBMD or vBMD measured at the same femoral region of interest [94]. The performance of DXA-based 3D modeling and FE simulations in terms of fracture risk prediction requires additional testing in prospective studies.

Effects of osteoporosis drugs on bone mass, FEA, and bone strength in preclinical studies

As part of regulatory submissions prior to approval of a new therapeutic agent, preclinical studies are required to demonstrate the safety of the treatment. Safety is assessed via comprehensive toxicity studies and by demonstrating a normal relationship between bone mass or density and biomechanical outcomes, which is interpreted to indicate that the treatment maintains normal bone “quality.” Preclinical studies that employ non-human primates may be particularly useful when trying to establish that bone strength estimates from CT-based FEA following pharmacologic intervention are valid and clinically meaningful. However, we found no published monkey studies comparing the effects of drugs on hip FEA vs actual strength. The only FEA studies reporting the

relationship between in vivo estimated strength and ex vivo experimental strength are those by Lee et al (vertebrae, denosumab) [95] and Cabal et al (radius, odanacatib) [96].

Preclinical studies have employed ovariectomized baboons (alendronate [97, 98]), rhesus monkeys (zoledronic acid [99], PTH (1-84) [100], odanacatib [96, 101, 102]), and cynomolgus monkeys (teriparatide [103, 104], ibandronate [105–107], denosumab [95, 98, 108], romosozumab [109], and abaloparatide [110]). Treatment durations ranged from 6 to 24 months. Depending on the study, outcomes included in vivo bone density measurements by DXA, pQCT, and/or HR-pQCT, along with ex vivo assessment of bone strength via mechanical testing of the vertebral body, femoral neck, femoral diaphysis, vertebral trabecular cores, and/or cortical beam specimens. Without exception, bone mass and bone mechanical properties were either maintained or increased by the treatments, and in all cases the expected bone mass to bone strength relationship was preserved, inferring no deficits in bone quality due to the treatment.

Focusing specifically on femoral strength, osteoporosis treatments have had either no effect or led to increased biomechanical properties of the femoral neck and/or the femoral diaphysis in ovariectomized non-human primates (Table 5). Specifically, the bisphosphonates alendronate and ibandronate had no effect on femoral neck strength but maintained a normal association between bone mass and bone strength. In comparison, denosumab led to increased femoral neck mechanical properties, with no effect on estimated cortical bone material properties at the femoral diaphysis. Treatment of OVX cynomolgus monkeys with denosumab (25 or 50 mg/kg/month) for 16 months led to increased stiffness of the femoral diaphysis (at both doses) and higher femoral neck stiffness in the higher dose denosumab group, while maintaining the expected bone mass vs. bone strength relationship [97].

Considering anabolic therapies, treatment of OVX cynomolgus monkeys for 18 months with teriparatide (1 or 5 $\mu\text{g}/\text{kg}/\text{day}$) led to higher femoral neck peak load versus vehicle-treated monkeys in both of the teriparatide-treated groups. Treatment of OVX rhesus monkeys for 16 months with PTH (1-84) at 5, 10, or 25 $\mu\text{g}/\text{kg}/\text{day}$ revealed no differences among groups in femoral neck stiffness or peak load, but a higher work to failures in the 10- and 25 $\mu\text{g}/\text{kg}/\text{day}$ groups when compared to vehicle-treated monkeys. In a study of the PTH analog abaloparatide, 9 to 18 years old cynomolgus monkeys were subjected to ovariectomy or sham surgery [110]. After 9 months without treatment, the OVX groups were treated with daily s.c. injections of either vehicle or abaloparatide (0.2, 1, or 5 $\mu\text{g}/\text{kg}/\text{day}$). There were no differences in femoral diaphysis or femoral neck biomechanical properties between groups, but abaloparatide maintained normal bone mass versus bone strength relationships for both the femoral neck and femoral diaphysis, consistent with maintenance of bone quality following abaloparatide treatment. In a

Table 5 Summary of selected non-human primate studies with osteoporosis drug treatment and mechanical testing outcomes

Drug	Animal model	Treatment duration and dose	Femoral diaphysis testing	Femoral neck testing	Maintained normal bone mass vs. bone strength relationship?	Reference
Alendronate	OVX baboon	24 months VEH, 0.05 or 0.25 mg/kg every 2 weeks	No differences among groups	No differences among groups	Yes	Balena et al., 1993 [97]
Zoledronic acid	OVX rhesus	17 months VEH, 0.5, 2.5, or 12.5 µg/kg/week	Not reported	Not reported	Not reported	Binkley et al., 1998 [99]
Ibandronate	OVX cynomolgus monkey	16 months VEH, 10, 30, or 150 µg/kg/month	Not reported	No differences among groups	Yes	Smith et al., 2003 [106]
Denosumab	OVX cynomolgus monkey	16 months VEH, 25 or 50 mg/kg/month	Stiffness higher in both denosumab groups vs VEH; no differences in estimated material properties	FN stiffness higher in 50 mg/kg dose group vs VEH; no difference in 25 mg/kg dose group	Yes	Ominsky et al., 2011 [111]
Teriparatide	OVX cynomolgus monkey	18 months VEH, 1 or 5 µg/kg/day	Not reported	FN failure load higher in PTH-treated (both doses) vs VEH	Yes	Sato et al., 2004 [112]
PTH (1-84)	OVX rhesus monkey	16 months VEH, 5, 10, or 25 µg/kg/day	Not reported	No difference in FN stiffness or peak load; higher FN work to failure in 10 and 25 µg/kg vs VEH	Yes	Fox et al., 2007 [100]
Abaloparatide	OVX cynomolgus monkey	16 months VEH, 0.2, 1, or 5 µg/kg/day	No differences in structural or estimated material properties	No differences between groups	Yes	Doyle et al., 2018 [110]
Romosozumab	OVX cynomolgus monkey	12 months VEH, 3 or 30 mg/kg	Peak load and stiffness higher in 30 mg/kg vs VEH; no difference in estimated material properties	FN peak load, stiffness, and energy to failure higher in 30 mg/kg vs VEH	Yes	Ominsky et al., 2017 [109]

OVX, ovariectomy; VEH, vehicle; FN, femoral neck

study of the monoclonal antibody to sclerostin, romosozumab [109], cynomolgus monkeys were subjected to ovariectomy, left untreated for 4 months and then assigned to treatment with vehicle, 3 mg/kg, or 30 mg/kg romosozumab for 12 months. Romosozumab treatment led to increased aBMD at the proximal femur, changes that translated into significant increases in bone strength in the high dose group in the femur diaphysis and femoral neck. The normal bone mass versus bone strength relationship was maintained in all groups, and there were no changes in estimated material properties at cortical bone sites.

Collectively these preclinical studies confirm that the expected bone mass to bone strength relationship is maintained for all currently approved osteoporosis therapies. This observation suggests that the empirical relationships between bone density and bone material properties used in the estimation of

bone strength by finite element analysis should be valid for both untreated individuals and those who have received pharmacologic treatment for osteoporosis.

Effects of osteoporosis treatment on FEA estimates of bone strength in clinical trials

The relationship between treatment-induced changes in aBMD and fracture risk has been controversial, with analyses from individual trials reporting that only small proportions of vertebral fracture risk reduction are explained by changes in spine aBMD while other analyses finding that the majority of the reduction in non-vertebral fracture risk is explained by increases in hip aBMD [21, 113–115]. The inconsistency in

these estimates is in part attributable to differences in methodology for estimating the proportion of treatment effect explained by changes in aBMD and/or wide confidence intervals in these estimates in trials with small changes in aBMD. However, a recent meta-analysis of published data from 38 placebo-controlled trials demonstrated a strong, significant association between the treatment-induced changes in aBMD and vertebral and hip fracture risk, with larger aBMD gains associated with greater fracture reduction [23].

The well-known disparity between large changes in spine BMD associated with sodium fluoride therapy and an observed increase in fracture risk was a major factor in regulatory agencies not accepting changes in BMD as a surrogate for fracture risk. Although failure of fluoride treatment to improve bone strength commensurate with BMD change was predicted by preclinical studies [116], currently, approval of new drugs for treatment of

osteoporosis still requires demonstration of fracture risk reduction in clinical studies of patients with osteoporosis.

Given their strong association with in vitro strength, CT-based estimates of bone strength via FEA may be useful for predicting the anti-fracture efficacy of osteoporosis therapies. Accordingly, changes in FEA estimates of strength in response to treatment with osteoporosis drugs have been evaluated in several small clinical studies or subsets of patients from large clinical trials [117–125]. Summaries of the results of such studies are presented in Table 6.

Most of the studies used a voxel-based method FEA [125] while other methodologies were used in some European-based trials [118, 119, 124]. In one study, different FEA methods were used to estimate hip and vertebral bone strength in the same set of QCT scans from a single study, providing highly comparable results [121, 124]. Altogether, the studies

Table 6 Summary of changes in FEA estimates of strength in response to treatment with osteoporosis drugs in small clinical studies or subsets of patients from large clinical trials

Drug	Patients	Number of Patients	Duration (months)	Skeletal site		Avg. Baseline BMD ([T-score] or g/cm ²)	Avg. Baseline (Newtons)	Change from baseline	Reference
				FEA	BMD				
Teriparatide	PMOP	28	18	VERT	LS	0.754	4351	21.0%	Keaveny et al., 2007 [126]
Alendronate		25				0.757	4592	3.7%	
PTH 1-84	PMOP	72	12	HIP	TH	0.748	2500-2600	2.1%	Keaveny et al., 2008 [120]
Alendronate		42				0.759		3.6%	
Combined		37				0.789		2.5%	
Ibandronate po	PMOP	47	12	HIP	TH	0.748	2410	2% (est)	Lewiecki et al., 2009 [122]
Placebo		46				0.759	2528	-3.9% (est)	
Ibandronate po		47		VERT	LS	0.789	4195	4% (est)	
Placebo		46				0.786	4017	-3.1% (est)	
Teriparatide	PMOP	44	24	VERT	LS	0.72	4333	28.1%	Graeff et al., 2009 [119]
Teriparatide	PMOP	27	18	HIP	TH	0.75	1930	5.4%	Keaveny et al., 2012 [127]
Alendronate		21				0.73	2020	0.9%	
Odanacatib	LBMD	109	24	HIP	TH	[-1.3]	3176	3.6% (est)	Brixen et al., 2013 [117]
Placebo		105				[-1.3]	3191	-2% (est)	
Odanacatib		109		VERT	LS	[-1.7]	3667	9.3% (est)	
Placebo		105				[-1.9]	3685	-5% (est)	
Denosumab	PMOP	51	36	HIP	TH	[-1.7]	2512	8.3%	Keaveny et al., 2014 [121]
Placebo		48				[-2.0]	2273	-5.6%	
Denosumab		51		VERT	LS	[-2.8]	2879	18.2%	
Placebo		48				[-2.8]	2841	-4.2%	
Denosumab	PMOP	51	36	HIP	TH	[-1.7]	2311	5.2%	Zysset et al., 2015 [124]
Placebo		47				[-2.0]	2107	-1.9%	
Denosumab		51		VERT	LS	[-2.8]	3070	17.4%	
Placebo		47				[-2.8]	2996	-3.3%	
Romozosumab	LBMD	9	12	HIP	TH	NA	NA	3.6%	Keaveny et al., 2017 [128]
Teriparatide		19						-0.7%	
Placebo		18						-0.1%	

FEA, finite element analysis; PMOP, postmenopausal osteoporosis; LBMD, low bone mineral density; BMD, bone mineral density; VERT, vertebra; TH, total hip; LS, lumbar spine; (est), changes from baseline estimated from figure in paper to match the reported change vs placebo; NA, not available

included treatment groups ranging in size from 3 to 109 subjects and followed patients for 6 to 36 months. Comparisons were made with placebo, another osteoporosis treatment or both.

Estimates of bone strength decreased modestly in each of the placebo groups. Increases in hip strength were observed with bisphosphonates and denosumab, but the changes were smaller than the changes in vertebral strength. The changes in hip strength in response to anabolic therapies were small and somewhat inconsistent. In the few studies in which treatment responses were reported at multiple time points, increases in FEA estimates of strength were greater during the first several months of therapy than during the second or third year of treatment. FEA changes upon stopping therapy have not been evaluated in any study.

Positive but modest associations between changes in FEA strength and aBMD changes were reported, with stronger correlations observed with changes in vBMD measurements. No study or collection of studies was large enough to describe the relationship between changes in estimates of strength and fracture risk reduction.

These studies document that osteoporosis therapies do have a positive impact on vertebral and femoral strength, consistent with the beneficial effects of treatment on fracture risk, suggesting that FEA could be of value in monitoring responses to osteoporosis therapies. Whether changes in FEA estimates of strength are better predictors of the effects of treatment on fracture incidence than are changes in aBMD remains to be determined. To know this will require collection of CT scans in many patients in large fracture endpoint trials. Unfortunately, few if any such fracture endpoint studies are on the horizon. One promising prospect is the recent validation of DXA-derived FEA analysis [77]. Such a technique might allow the analysis of the large storehouse of DXA scans collected in the many previous clinical fracture endpoint studies.

Conclusions and perspective

Bone mineral density explains a large proportion of the femoral strength, as demonstrated both *ex vivo* in human cadaveric and monkey samples, and *in vivo* by the inverse relationship between aBMD and fracture risk. Estimation of hip strength by CT-based FEA is also strongly correlated with *ex vivo* femoral strength, and *in vivo* CT-derived estimations of bone strength are as good or better than aBMD to predict fracture risk. Additional studies are needed to determine the optimal approach for FEA-based bone strength assessments, including exploration of hip strength using various loading configurations/directions and then considering the weakest estimate as the femoral strength, and by considering individual impact loads based on anthropometric variables. Further areas for possible

improvement of current FEA approaches to predict femoral strength and hip fracture include the incorporation of trabecular orientation, improved definition and modeling of the cortex and consideration of age-related changes in bone tissue ductility.

Importantly, changes in aBMD in response to a variety of osteoporosis drugs are strongly correlated with breaking strength in animal models, as commonly evaluated at the mid-shaft femur (although rarely at the hip), and changes in aBMD from clinical trials explain a substantial proportion of the reduction in hip fracture risk. Although the effects of osteoporosis drugs on FEA-derived hip strength have been evaluated for most drugs, due to the relatively small sample size for these studies, changes in hip strength by CT-FEA have not been correlated with fracture risk reduction. For this purpose, a (very) large clinical trial comparing the effects of various drugs on changes in BMD and structure at the hip evaluated by CT and hip fracture incidence would be necessary—which is unlikely to ever be conducted.

Thus, due to the observations that both hip aBMD and FEA-estimated femoral strength are good predictors of fracture risk, they are excellent candidates to replace fracture endpoints in clinical trials. Whereas a large body of data are available to test whether aBMD could be validated as a surrogate endpoint for fractures in future clinical trials [22], unfortunately FEA strength assessments were conducted in a relatively small subset of subjects in clinical trials. Nevertheless, considering the evidence that bone strength from FEA is well correlated to *ex vivo* strength and predicts fracture risk, there is no reason to believe that this correlation should not exist in treated patients. Ultimately, validation of hip aBMD or FEA-derived hip strength as a surrogate endpoint for fracture could lead to shorter and less expensive clinical trials in the near future, thereby spurring innovation and prompting the development of new drugs and procedures which might otherwise not be investigated due the high cost of conducting a clinical trial with fracture outcomes.

Acknowledgments We are grateful to the Committee of Scientific Advisors of the International Osteoporosis Foundation for their review and endorsement of this paper.

Preparation of this manuscript was supported by an unrestricted grant from AgNovos to the International Osteoporosis Foundation. The sponsor did not have any role in preparation, review, or approval of the manuscript.

Compliance with ethical standards

Conflict of interest MLB reports consulting fees from AgNovos Healthcare and Keros Therapeutics and research funding from Amgen and Radius and from the Foundation for NIH (FNIH) Bone Quality Project. CCG reports consulting fees from AgNovos Healthcare and Mindways Software, Inc. and research funding from AgNovos. SLF reports consulting and/or speaker honoraria from Amgen, UCB, Lilly, Labatec, Agnovos, Pfizer. MRM reports consulting fees from Amgen and Myovant and honorarium from Amgen. PhZ reports research funding from Mereo BioPharma and Nobel Biocare. EB and DP have nothing to declare.

References

- Johnell O, Kanis JA (2006) An estimate of the worldwide prevalence and disability associated with osteoporotic fractures. *Osteoporos Int* 17:1726–1733
- Gullberg B, Johnell O, Kanis JA (1997) World-wide projections for hip fracture. *Osteoporos Int* 7:407–413
- Cooper C, Campion G, Melton LJ 3rd (1992) Hip fractures in the elderly: a world-wide projection. *Osteoporos Int* 2:285–289
- Hernlund E, Svedbom A, Ivergard M, Compston J, Cooper C, Stenmark J, McCloskey EV, Jonsson B, Kanis JA (2013) Osteoporosis in the European Union: medical management, epidemiology and economic burden. A report prepared in collaboration with the International Osteoporosis Foundation (IOF) and the European Federation of Pharmaceutical Industry Associations (EFPIA). *Arch Osteoporos* 8:136
- Cummings SR, Black DM, Rubin SM (1989) Lifetime risks of hip, Colles', or vertebral fracture and coronary heart disease among white postmenopausal women. *Arch Intern Med* 149:2445–2448
- Kanis JA, Johnell O, Oden A, Sembo I, Redlund-Johnell I, Dawson A, De Laet C, Jonsson B (2000) Long-term risk of osteoporotic fracture in Malmo. *Osteoporos Int* 11:669–674
- Melton LJ 3rd, Chrischilles EA, Cooper C, Lane AW, Riggs BL (1992) Perspective. How many women have osteoporosis? *J Bone Miner Res* 7:1005–1010
- van Staa TP, Dennison EM, Leufkens HG, Cooper C (2001) Epidemiology of fractures in England and Wales. *Bone* 29:517–522
- Ryg J, Rejnmark L, Overgaard S, Brixen K, Vestergaard P (2009) Hip fracture patients at risk of second hip fracture: a nationwide population-based cohort study of 169,145 cases during 1977–2001. *J Bone Miner Res* 24:1299–1307
- Bynum JPW, Bell JE, Cantu RV, Wang Q, McDonough CM, Carmichael D, Tosteson TD, Tosteson ANA (2016) Second fractures among older adults in the year following hip, shoulder, or wrist fracture. *Osteoporos Int* 27:2207–2215
- Kanis JA, Johansson H, Oden A et al (2018) Characteristics of recurrent fractures. *Osteoporos Int* 29:1747–1757
- Shah A, Prieto-Alhambra D, Hawley S, Delmestri A, Lippett J, Cooper C, Judge A, Javaid MK, team REs (2017) Geographic variation in secondary fracture prevention after a hip fracture during 1999–2013: a UK study. *Osteoporos Int* 28:169–178
- Yusuf AA, Matlon TJ, Grauer A, Barron R, Chandler D, Peng Y (2016) Utilization of osteoporosis medication after a fragility fracture among elderly Medicare beneficiaries. *Arch Osteoporos* 11:31
- Akesson K, Marsh D, Mitchell PJ, AR ML, Stenmark J, Pierroz DD, Kyer C, Cooper C, Group IOFFW (2013) Capture the Fracture: a Best Practice Framework and global campaign to break the fragility fracture cycle. *Osteoporos Int* 24:2135–2152
- Javaid MK, Kyer C, Mitchell PJ et al (2015) Effective secondary fracture prevention: implementation of a global benchmarking of clinical quality using the IOF Capture the Fracture(R) Best Practice Framework tool. *Osteoporos Int* 26:2573–2578
- Marsh D, Akesson K, Beaton DE et al (2011) Coordinator-based systems for secondary prevention in fragility fracture patients. *Osteoporos Int* 22:2051–2065
- Marshall D, Johnell O, Wedel H (1996) Meta-analysis of how well measures of bone mineral density predict occurrence of osteoporotic fractures. *BMJ* 312:1254–1259
- Johannesdottir F, Aspelund T, Reeve J, Poole KE, Sigurdsson S, Harris TB, Gudnason VG, Sigurdsson G (2013) Similarities and differences between sexes in regional loss of cortical and trabecular bone in the mid-femoral neck: the AGES-Reykjavik longitudinal study. *J Bone Miner Res* 28:2165–2176
- Zebaze RM, Ghasem-Zadeh A, Bohte A, Iuliano-Burns S, Mirans M, Price RI, Mackie EJ, Seeman E (2010) Intracortical remodeling and porosity in the distal radius and post-mortem femurs of women: a cross-sectional study. *Lancet* 375:1729–1736
- Keaveny TM, Kopperdahl DL, Melton LJ 3rd, Hoffmann PF, Amin S, Riggs BL, Khosla S (2010) Age-dependence of femoral strength in white women and men. *J Bone Miner Res* 25:994–1001
- Austin M, Yang YC, Vittinghoff E et al (2012) Relationship between bone mineral density changes with denosumab treatment and risk reduction for vertebral and nonvertebral fractures. *J Bone Miner Res* 27:687–693
- Black DM (2018) Change in BMD as a Surrogate for Fracture Risk Reduction in Osteoporosis Trials: Results from Pooled, Individual-level Patient Data from the FNIH Bone Quality Project Available at <http://www.asbmr.org/ItineraryBuilder/PresentationDetails.aspx?pid=6f3d7ce1-cd5b-41f0-862b-42733a02c150&ptag=AuthorDetail&aid=00000000-0000-0000-0000-000000000000> Accessed December 4, 2018
- Bouxein ML, Eastell R, Lui LY et al (2019) Change in Bone Density and Reduction in Fracture Risk: A Meta-Regression of Published Trials. *J Bone Miner Res* 34:632–642
- Lochmuller EM, Zeller JB, Kaiser D, Eckstein F, Landgraf J, Putz R, Steldinger R (1998) Correlation of femoral and lumbar DXA and calcaneal ultrasound, measured in situ with intact soft tissues, with the in vitro failure loads of the proximal femur. *Osteoporos Int* 8:591–598
- Johannesdottir F, Thrall E, Muller J, Keaveny TM, Kopperdahl DL, Bouxein ML (2017) Comparison of non-invasive assessments of strength of the proximal femur. *Bone* 105:93–102
- Beck TJ, Ruff CB, Warden KE, Scott WW Jr, Rao GU (1990) Predicting femoral neck strength from bone mineral data. A structural approach. *Invest Radiol* 25:6–18
- Smith MD, Cody DD, Goldstein SA, Cooperman AM, Matthews LS, Flynn MJ (1992) Proximal femoral bone density and its correlation to fracture load and hip-screw penetration load. *Clin Orthop Relat Res* 244:251
- Cody DD, Gross GJ, Hou FJ, Spencer HJ, Goldstein SA, Fyhrie DP (1999) Femoral strength is better predicted by finite element models than QCT and DXA. *J Biomech* 32:1013–1020
- Keyak JH (2001) Improved prediction of proximal femoral fracture load using nonlinear finite element models. *Med Eng Phys* 23:165–173
- Keyak JH, Rossi SA, Jones KA, Les CM, Skinner HB (2001) Prediction of fracture location in the proximal femur using finite element models. *Med Eng Phys* 23:657–664
- Kukla C, Gaebler C, Pichl RW, Prokesch R, Heinze G, Heinz T (2002) Predictive geometric factors in a standardized model of femoral neck fracture. Experimental study of cadaveric human femurs. *Injury* 33:427–433
- Bessho M, Ohnishi I, Matsuyama J, Matsumoto T, Imai K, Nakamura K (2007) Prediction of strength and strain of the proximal femur by a CT-based finite element method. *J Biomech* 40:1745–1753
- Cristofolini L, Juszczak M, Martelli S, Taddei F, Viceconti M (2007) In vitro replication of spontaneous fractures of the proximal human femur. *J Biomech* 40:2837–2845
- Duchemin L, Mitton D, Jolivet E, Bousson V, Laredo J, Skalli W (2008) An anatomical subject-specific FE-model for hip fracture load prediction. *Comput Methods Biomech Biomed Engin* 11:105–111
- Dall'Ara E, Luisier B, Schmidt R, Pretterklieber M, Kainberger F, Zysset P, Pahr D (2013) DXA predictions of human femoral

- mechanical properties depend on the load configuration. *Med Eng Phys* 35:1564–1572 discussion 1564
36. Courtney AC, Wachtel EF, Myers ER, Hayes WC (1994) Effects of loading rate on strength of the proximal femur. *Calcif Tissue Int* 55:53–58
 37. Pinilla TP, Boardman KC, Bouxsein ML, Myers ER, Hayes WC (1996) Impact direction from a fall influences the failure load of the proximal femur as much as age-related bone loss. *Calcif Tissue Int* 58:231–235
 38. Cheng XG, Lowet G, Boonen S, Nicholson PH, Brys P, Nijs J, Dequeker J (1997) Assessment of the strength of proximal femur in vitro: relationship to femoral bone mineral density and femoral geometry. *Bone* 20:213–218
 39. Pulkkinen P, Eckstein F, Lochmuller EM, Kuhn V, Jamsa T (2006) Association of geometric factors and failure load level with the distribution of cervical vs. trochanteric hip fractures. *J Bone Miner Res* 21:895–901
 40. Manske SL, Liu-Ambrose T, Cooper DM, Kontulainen S, Guy P, Forster BB, McKay HA (2009) Cortical and trabecular bone in the femoral neck both contribute to proximal femur failure load prediction. *Osteoporos Int* 20:445–453
 41. de Bakker PM, Manske SL, Ebacher V, Oxland TR, Crompton PA, Guy P (2009) During sideways falls proximal femur fractures initiate in the superolateral cortex: evidence from high-speed video of simulated fractures. *J Biomech* 42:1917–1925
 42. Roberts BJ, Thrall E, Muller JA, Bouxsein ML (2010) Comparison of hip fracture risk prediction by femoral aBMD to experimentally measured factor of risk. *Bone* 46:742–746
 43. Dragomir-Daescu D, Op Den Buijs J, McEligot S, Dai Y, Entwistle RC, Salas C, Melton LJ 3rd, Bennet KE, Khosla S, Amin S (2011) Robust QCT/FEA models of proximal femur stiffness and fracture load during a sideways fall on the hip. *Ann Biomed Eng* 39:742–755
 44. Koivumaki JE, Thevenot J, Pulkkinen P, Kuhn V, Link TM, Eckstein F, Jamsa T (2012) Ct-based finite element models can be used to estimate experimentally measured failure loads in the proximal femur. *Bone* 50:824–829
 45. Nishiyama KK, Gilchrist S, Guy P, Crompton P, Boyd SK (2013) Proximal femur bone strength estimated by a computationally fast finite element analysis in a sideways fall configuration. *J Biomech* 46:1231–1236
 46. Gebauer M, Stark O, Vettorazzi E, Grifka J, Puschel K, Amling M, Beckmann J (2014) DXA and pQCT predict pertrochanteric and not femoral neck fracture load in a human side-impact fracture model. *J Orthop Res* 32:31–38
 47. Gilchrist S, Nishiyama KK, de Bakker P, Guy P, Boyd SK, Oxland T, Crompton PA (2014) Proximal femur elastic behaviour is the same in impact and constant displacement rate fall simulation. *J Biomech* 47:3744–3749
 48. Zani L, Erani P, Grassi L, Taddei F, Cristofolini L (2015) Strain distribution in the proximal Human femur during in vitro simulated sideways fall. *J Biomech* 48:2130–2143
 49. Varga P, Schwiedrzik J, Zysset PK, Fliri-Hofmann L, Widmer D, Gueorguiev B, Blauth M, Windolf M (2016) Nonlinear quasi-static finite element simulations predict in vitro strength of human proximal femora assessed in a dynamic sideways fall setup. *J Mech Behav Biomed Mater* 57:116–127
 50. Pottecher P, Engelke K, Duchemin L et al (2016) Prediction of Hip Failure Load: In Vitro Study of 80 Femurs Using Three Imaging Methods and Finite Element Models-The European Fracture Study (EFFECT). *Radiology* 280:837–847
 51. Dragomir-Daescu D, Rossman TL, Rezaei A, Carlson KD, Kallmes DF, Skinner JA, Khosla S, Amin S (2018) Factors associated with proximal femur fracture determined in a large cadaveric cohort. *Bone* 116:196–202
 52. Eckstein F, Wunderer C, Boehm H, Kuhn V, Priemel M, Link TM, Lochmuller EM (2004) Reproducibility and side differences of mechanical tests for determining the structural strength of the proximal femur. *J Bone Miner Res* 19:379–385
 53. Dalen N, Hellstrom LG, Jacobson B (1976) Bone mineral content and mechanical strength of the femoral neck. *Acta Orthop Scand* 47:503–508
 54. Leichter I, Margulies JY, Weinreb A, Mizrahi J, Robin GC, Conforty B, Makin M, Bloch B (1982) The relationship between bone density, mineral content, and mechanical strength in the femoral neck. *Clin Orthop Relat Res* 272–281
 55. Esses SL, Lotz JC, Hayes WC (1989) Biomechanical properties of the proximal femur determined in vitro by single-energy quantitative computed tomography. *J Bone Miner Res* 4:715–722
 56. Link TM, Vieth V, Langenberg R, Meier N, Lotter A, Newitt D, Majumdar S (2003) Structure analysis of high resolution magnetic resonance imaging of the proximal femur: in vitro correlation with biomechanical strength and BMD. *Calcif Tissue Int* 72:156–165
 57. Abraham AC, Agarwalla A, Yadavalli A, McAndrew C, Liu JY, Tang SY (2015) Multiscale Predictors of Femoral Neck In Situ Strength in Aging Women: Contributions of BMD, Cortical Porosity, Reference Point Indentation, and Nonenzymatic Glycation. *J Bone Miner Res* 30:2207–2214
 58. Lotz JC, Hayes WC (1990) The use of quantitative computed tomography to estimate risk of fracture of the hip from falls. *J Bone Joint Surg Am* 72:689–700
 59. Keyak JH, Rossi SA, Jones KA, Skinner HB (1998) Prediction of femoral fracture load using automated finite element modeling. *J Biomech* 31:125–133
 60. Pithioux M, Chabrand P, Hochard C, Champsaur P (2011) Improved femoral neck fracture predictions using anisotropic failure criteria models. *Journal of Mechanics in Medicine and Biology* 11:1333–1346
 61. Dall'Ara E, Luisier B, Schmidt R, Kainberger F, Zysset P, Pahr D (2013) A nonlinear QCT-based finite element model validation study for the human femur tested in two configurations in vitro. *Bone* 52:27–38
 62. Luisier B, Dall'Ara E, Pahr DH (2014) Orthotropic HR-pQCT-based FE models improve strength predictions for stance but not for side-way fall loading compared to isotropic QCT-based FE models of human femurs. *J Mech Behav Biomed Mater* 32:287–299
 63. Hamblin R, Allaoui S (2013) A robust 3D finite element simulation of human proximal femur progressive fracture under stance load with experimental validation. *Ann Biomed Eng* 41:2515–2527
 64. Langton CM, Pisharody S, Keyak JH (2009) Comparison of 3D finite element analysis derived stiffness and BMD to determine the failure load of the excised proximal femur. *Med Eng Phys* 31:668–672
 65. Enns-Bray WS, Owoc JS, Nishiyama KK, Boyd SK (2014) Mapping anisotropy of the proximal femur for enhanced image based finite element analysis. *J Biomech* 47:3272–3278
 66. Thevenot J, Koivumaki J, Kuhn V, Eckstein F, Jamsa T (2014) A novel methodology for generating 3D finite element models of the hip from 2D radiographs. *J Biomech* 47:438–444
 67. Schileo E, Balistreri L, Grassi L, Cristofolini L, Taddei F (2014) To what extent can linear finite element models of human femora predict failure under stance and fall loading configurations? *J Biomech* 47:3531–3538
 68. Nawathe S, Akhlaghpour H, Bouxsein ML, Keaveny TM (2014) Microstructural failure mechanisms in the human proximal femur for sideways fall loading. *J Bone Miner Res* 29:507–515
 69. Ariza O, Gilchrist S, Widmer RP, Guy P, Ferguson SJ, Crompton PA, Helgason B (2015) Comparison of explicit finite element and mechanical simulation of the proximal femur during dynamic drop-tower testing. *J Biomech* 48:224–232

70. Morgan EF, Bouxsein ML (2005) Use of finite element analysis to assess bone strength. *BoneKey-Osteovision* 2:8–19
71. Luo Y, Ferdous Z, Leslie WD (2013) Precision study of DXA-based patient-specific finite element modeling for assessing hip fracture risk. *Int J Numer Method Biomed Eng* 29:615–629
72. Yang L, Palermo L, Black DM, Eastell R (2014) Prediction of incident hip fracture with the estimated femoral strength by finite element analysis of DXA Scans in the study of osteoporotic fractures. *J Bone Miner Res* 29:2594–2600
73. Keaveny TM (2010) Biomechanical computed tomography-non-invasive bone strength analysis using clinical computed tomography scans. *Ann N Y Acad Sci* 1192:57–65
74. Grassi L, Vaananen SP, Ristinmaa M, Jurvelin JS, Isaksson H (2017) Prediction of femoral strength using 3D finite element models reconstructed from DXA images: validation against experiments. *Biomech Model Mechanobiol* 16:989–1000
75. Humbert L, Martelli Y, Fonolla R, Steghofer M, Di Gregorio S, Malouf J, Romera J, Barquero LM (2017) 3D-DXA: Assessing the Femoral Shape, the Trabecular Macrostructure and the Cortex in 3D from DXA images. *IEEE Trans Med Imaging* 36:27–39
76. Cody DD, Hou FJ, Divine GW, Fyhrie DP (2000) Short term in vivo precision of proximal femoral finite element modeling. *Ann Biomed Eng* 28:408–414
77. Dall'Ara E, Eastell R, Viceconti M, Pahr D, Yang L (2016) Experimental validation of DXA-based finite element models for prediction of femoral strength. *J Mech Behav Biomed Mater* 63:17–25
78. Whitmarsh T, Humbert L, De Craene M, Del Rio Barquero LM, Frangi AF (2011) Reconstructing the 3D shape and bone mineral density distribution of the proximal femur from dual-energy X-ray absorptiometry. *IEEE Trans Med Imaging* 30:2101–2114
79. van den Munckhof S, Zadpoor AA (2014) How accurately can we predict the fracture load of the proximal femur using finite element models? *Clin Biomech (Bristol, Avon)* 29:373–380
80. Zysset PK, Dall'ara E, Varga P, Pahr DH (2013) Finite element analysis for prediction of bone strength. *Bonekey Rep* 2:386
81. Naylor KE, McCloskey EV, Eastell R, Yang L (2013) Use of DXA-based finite element analysis of the proximal femur in a longitudinal study of hip fracture. *J Bone Miner Res* 28:1014–1021
82. Orwoll ES, Marshall LM, Nielson CM et al (2009) Finite element analysis of the proximal femur and hip fracture risk in older men. *J Bone Miner Res* 24:475–483
83. Kopperdahl DL, Aspelund T, Hoffmann PF, Sigurdsson S, Siggeirsdottir K, Harris TB, Gudnason V, Keaveny TM (2014) Assessment of incident spine and hip fractures in women and men using finite element analysis of CT scans. *J Bone Miner Res* 29:570–580
84. Adams AL, Fischer H, Kopperdahl DL et al (2018) Osteoporosis and Hip Fracture Risk From Routine Computed Tomography Scans: The Fracture, Osteoporosis, and CT Utilization Study (FOCUS). *J Bone Miner Res* 33:1291–1301
85. Leslie WD, Luo Y, Yang S, Goertzen AL, Ahmed S, Delubac I, Lix LM (2019) Fracture Risk Indices From DXA-Based Finite Element Analysis Predict Incident Fractures Independently From FRAX: The Manitoba BMD Registry. *J Clin Densitom*
86. Bouxsein ML (2013) Overview of bone structure and strength Genetics of Bone Biology and Skeletal Disease, Elsevier, 1st edition
87. Keyak JH, Sigurdsson S, Karlsdottir GS et al (2013) Effect of finite element model loading condition on fracture risk assessment in men and women: the AGES-Reykjavik study. *Bone* 57:18–29
88. Khoo BC, Brown K, Cann K, Zhu K, Henzell S, Low V, Gustafsson S, Price RI, Prince RL (2009) Comparison of QCT-derived and DXA-derived areal bone mineral density and T scores. *Osteoporos Int* 20:1539–1545
89. Lee DC, Hoffmann PF, Kopperdahl DL, Keaveny TM (2017) Phantomless calibration of CT scans for measurement of BMD and bone strength-Inter-operator reanalysis precision. *Bone* 103:325–333
90. Wang X, Sanyal A, Cawthon PM et al (2012) Prediction of new clinical vertebral fractures in elderly men using finite element analysis of CT scans. *J Bone Miner Res* 27:808–816
91. Falcinelli C, Schileo E, Balistreri L et al (2014) Multiple loading conditions analysis can improve the association between finite element bone strength estimates and proximal femur fractures: a preliminary study in elderly women. *Bone* 67:71–80
92. Yang S, Leslie WD, Luo Y, Goertzen AL, Ahmed S, Ward LM, Delubac I, Lix LM (2018) Automated DXA-based finite element analysis for hip fracture risk stratification: a cross-sectional study. *Osteoporos Int* 29:191–200
93. Vaananen SP, Grassi L, Flivik G, Jurvelin JS, Isaksson H (2015) Generation of 3D shape, density, cortical thickness and finite element mesh of proximal femur from a DXA image. *Med Image Anal* 24:125–134
94. Ruiz Wills C, Olivares AL, Tassani S, Ceresa M, Zimmer V, Gonzalez Ballester MA, Del Rio LM, Humbert L, Noailly J (2019) 3D patient-specific finite element models of the proximal femur based on DXA towards the classification of fracture and non-fracture cases. *Bone* 121:89–99
95. Lee DC, Varela A, Kostenuik PJ, Ominsky MS, Keaveny TM (2016) Finite Element Analysis of Denosumab Treatment Effects on Vertebral Strength in Ovariectomized Cynomolgus Monkeys. *J Bone Miner Res* 31:1586–1595
96. Cabal A, Jayakar RY, Sardesai S et al (2013) High-resolution peripheral quantitative computed tomography and finite element analysis of bone strength at the distal radius in ovariectomized adult rhesus monkey demonstrate efficacy of odanacatib and differentiation from alendronate. *Bone* 56:497–505
97. Balena R, Toolan BC, Shea M et al (1993) The effects of 2-year treatment with the aminobisphosphonate alendronate on bone metabolism, bone histomorphometry, and bone strength in ovariectomized nonhuman primates. *J Clin Invest* 92:2577–2586
98. Kostenuik PJ, Smith SY, Samadfar M, Jolette J, Zhou L, Ominsky MS (2015) Effects of denosumab, alendronate, or denosumab following alendronate on bone turnover, calcium homeostasis, bone mass and bone strength in ovariectomized cynomolgus monkeys. *J Bone Miner Res* 30:657–669
99. Binkley N, Kimmel D, Bruner J, Haffa A, Davidowitz B, Meng C, Schaffer V, Green J (1998) Zoledronate prevents the development of absolute osteopenia following ovariectomy in adult rhesus monkeys. *J Bone Miner Res* 13:1775–1782
100. Fox J, Miller MA, Newman MK, Turner CH, Recker RR, Smith SY (2007) Treatment of skeletally mature ovariectomized rhesus monkeys with PTH(1-84) for 16 months increases bone formation and density and improves trabecular architecture and biomechanical properties at the lumbar spine. *J Bone Miner Res* 22:260–273
101. Cusick T, Chen CM, Pennypacker BL, Pickarski M, Kimmel DB, Scott BB, Duong LT (2012) Odanacatib treatment increases hip bone mass and cortical thickness by preserving endocortical bone formation and stimulating periosteal bone formation in the ovariectomized adult rhesus monkey. *J Bone Miner Res* 27:524–537
102. Masarachia PJ, Pennypacker BL, Pickarski M et al (2012) Odanacatib reduces bone turnover and increases bone mass in the lumbar spine of skeletally mature ovariectomized rhesus monkeys. *J Bone Miner Res* 27:509–523
103. Burr DB, Hirano T, Turner CH, Hotchkiss C, Brommage R, Hock JM (2001) Intermittently administered human parathyroid hormone(1-34) treatment increases intracortical bone turnover and porosity without reducing bone strength in the humerus of ovariectomized cynomolgus monkeys. *J Bone Miner Res* 16:157–165

104. Turner CH, Burr DB, Hock JM, Brommage R, Sato M (2001) The effects of PTH (1-34) on bone structure and strength in ovariectomized monkeys. *Adv Exp Med Biol* 496:165–179
105. Bauss F, Lalla S, Endeley R, Hothorn LA (2002) Effects of treatment with ibandronate on bone mass, architecture, biomechanical properties, and bone concentration of ibandronate in ovariectomized aged rats. *J Rheumatol* 29:2200–2208
106. Smith SY, Recker RR, Hannan M, Muller R, Bauss F (2003) Intermittent intravenous administration of the bisphosphonate ibandronate prevents bone loss and maintains bone strength and quality in ovariectomized cynomolgus monkeys. *Bone* 32:45–55
107. Muller R, Hannan M, Smith SY, Bauss F (2004) Intermittent ibandronate preserves bone quality and bone strength in the lumbar spine after 16 months of treatment in the ovariectomized cynomolgus monkey. *J Bone Miner Res* 19:1787–1796
108. Kostenuik PJ, Smith SY, Jollette J, Schroeder J, Pyrah I, Ominsky MS (2011) Decreased bone remodeling and porosity are associated with improved bone strength in ovariectomized cynomolgus monkeys treated with denosumab, a fully human RANKL antibody. *Bone* 49:151–161
109. Ominsky MS, Boyd SK, Varela A et al (2017) Romosozumab Improves Bone Mass and Strength While Maintaining Bone Quality in Ovariectomized Cynomolgus Monkeys. *J Bone Miner Res* 32:788–801
110. Doyle N, Varela A, Haile S, Guldborg R, Kostenuik PJ, Ominsky MS, Smith SY, Hattersley G (2018) Abaloparatide, a novel PTH receptor agonist, increased bone mass and strength in ovariectomized cynomolgus monkeys by increasing bone formation without increasing bone resorption. *Osteoporos Int* 29:685–697
111. Ominsky MS, Stouch B, Schroeder J, Pyrah I, Stolina M, Smith SY, Kostenuik PJ (2011) Denosumab, a fully human RANKL antibody, reduced bone turnover markers and increased trabecular and cortical bone mass, density, and strength in ovariectomized cynomolgus monkeys. *Bone* 49:162–173
112. Sato M, Westmore M, Ma YL, Schmidt A, Zeng QQ, Glass EV, Vahle J, Brommage R, Jerome CP, Turner CH (2004) Teriparatide [PTH(1-34)] strengthens the proximal femur of ovariectomized nonhuman primates despite increasing porosity. *J Bone Miner Res* 19:623–629
113. Cummings SR, Karpf DB, Harris F, Genant HK, Ensrud K, LaCroix AZ, Black DM (2002) Improvement in spine bone density and reduction in risk of vertebral fractures during treatment with antiresorptive drugs. *Am J Med* 112:281–289
114. Delmas PD, Seeman E (2004) Changes in bone mineral density explain little of the reduction in vertebral or nonvertebral fracture risk with anti-resorptive therapy. *Bone* 34:599–604
115. Watts NB, Geusens P, Barton IP, Felsenberg D (2005) Relationship between changes in BMD and nonvertebral fracture incidence associated with risedronate: reduction in risk of nonvertebral fracture is not related to change in BMD. *J Bone Miner Res* 20:2097–2104
116. Turner CH, Garetto LP, Dunipace AJ, Zhang W, Wilson ME, Grynblas MD, Chachra D, McClintock R, Peacock M, Stookey GK (1997) Fluoride treatment increased serum IGF-1, bone turnover, and bone mass, but not bone strength, in rabbits. *Calcif Tissue Int* 61:77–83
117. Brixen K, Chapurlat R, Cheung AM et al (2013) Bone density, turnover, and estimated strength in postmenopausal women treated with odanacatib: a randomized trial. *J Clin Endocrinol Metab* 98:571–580
118. Graeff C, Campbell GM, Pena J, Borggrefe J, Padhi D, Kaufman A, Chang S, Libanati C, Gluer CC (2015) Administration of romosozumab improves vertebral trabecular and cortical bone as assessed with quantitative computed tomography and finite element analysis. *Bone* 81:364–369
119. Graeff C, Chevalier Y, Charlebois M, Varga P, Pahr D, Nickelsen TN, Morlock MM, Gluer CC, Zysset PK (2009) Improvements in vertebral body strength under teriparatide treatment assessed in vivo by finite element analysis: results from the EUROFORS study. *J Bone Miner Res* 24:1672–1680
120. Keaveny TM, Hoffmann PF, Singh M, Palermo L, Bilezikian JP, Greenspan SL, Black DM (2008) Femoral bone strength and its relation to cortical and trabecular changes after treatment with PTH, alendronate, and their combination as assessed by finite element analysis of quantitative CT scans. *J Bone Miner Res* 23:1974–1982
121. Keaveny TM, McClung MR, Genant HK et al (2014) Femoral and vertebral strength improvements in postmenopausal women with osteoporosis treated with denosumab. *J Bone Miner Res* 29:158–165
122. Lewiecki EM, Keaveny TM, Kopperdahl DL, Genant HK, Engelke K, Fuerst T, Kivitz A, Davies RY, Fitzpatrick LA (2009) Once-monthly oral ibandronate improves biomechanical determinants of bone strength in women with postmenopausal osteoporosis. *J Clin Endocrinol Metab* 94:171–180
123. Muschitz C, Kocijan R, Pahr D, Patsch JM, Amrein K, Misof BM, Kaider A, Resch H, Pietschmann P (2015) Ibandronate increases sclerostin levels and bone strength in male patients with idiopathic osteoporosis. *Calcif Tissue Int* 96:477–489
124. Zysset P, Pahr D, Engelke K et al (2015) Comparison of proximal femur and vertebral body strength improvements in the FREEDOM trial using an alternative finite element methodology. *Bone* 81:122–130
125. Keaveny TM, Crittenden DB, Bolognese MA et al (2015) Romosozumab improves strength at the lumbar spine and hip in postmenopausal women with low bone mass compared with teriparatide. *J Bone Miner Res* 28(Suppl 1):abstract 1143
126. Keaveny TM, Donley DW, Hoffmann PF, Mitlak BH, Glass EV, San Martin JA (2007) Effects of teriparatide and alendronate on vertebral strength as assessed by finite element modeling of QCT scans in women with osteoporosis. *J Bone Miner Res* 22:149–157
127. Keaveny TM, McClung MR, Wan X, Kopperdahl DL, Mitlak BH, Krohn K (2012) Femoral strength in osteoporotic women treated with teriparatide or alendronate. *Bone* 50:165–170
128. Keaveny TM, Crittenden DB, Bolognese MA et al (2017) Greater Gains in Spine and Hip Strength for Romosozumab Compared With Teriparatide in Postmenopausal Women With Low Bone Mass. *J Bone Miner Res* 32:1956–1962

Publisher's note Springer Nature remains neutral with regard to jurisdictional claims in published maps and institutional affiliations.